Proc. Indian Acad. Sci. (Earth Planet. Sci.) Vol. 105, No. 4, December 1996, pp. 413–429.

Straightforward inversion scheme (SIS) for one-dimensional magnetotelluric data

P K GUPTA[1], SRI NIWAS[1] and V K GAUR[2]

[1]Department of Earth Sciences, University of Roorkee, Roorkee 247 667, India.
[2]Center for Mathematical Modelling and Computer Simulation, National Aerospace Laboratories, Bangalore 560 037, India

MS received 19 March 1996; revised 5 June 1996

Abstract This paper presents a Straightforward Inversion Scheme (SIS) for interpreting one-dimensional magnetotelluric sounding data. The basic steps of SIS are (i) parameterization of the layered model such that the layer thickness, expressed in units of its skin depth, is a constant (α); (ii) expansion of the reflection function at each interface as a power series in parameter $u = \exp(-2(1+j)\alpha\sqrt{f})$; (iii) development of a recurrence relation between the coefficients of the same powers of u in the power series of reflection functions of any two successive layers; (iv) estimation of the impedance power series coefficients using regressed minimum norm estimator; and (v) evaluation of layer resistivities and thicknesses using the inverse recurrence relation. The power of SIS is established by inverting four synthetic data sets and two field data sets. The effect of noise is extensively studied on a synthetic data set, deliberately corrupted with increasing levels of Gaussian random noise up to 25%. It is found that the scheme can retrieve broad features of the true model even with noise levels as high as 25%. On the basis of findings of different experiments conducted on SIS, it is concluded that SIS is an efficient, robust algorithm with high resolving power. Further, being linear, it is non-iterative and it dispenses with the requirement of having to choose an initial guess model.

Keywords Inversion; MT data.

1. Introduction

Electrical properties of the earth materials exhibit the widest range of variations spanning 8–10 orders of magnitude. Electrical resistivity is, therefore, a good indicator of their distinctive character and a knowledge of its distribution at different depths provides a direct clue to the way different kinds of materials are placed in the deeper regions. Magnetotelluric sounding is, therefore, often employed to elucidate the nature and texture of rock formation at depth. This information, in turn, is made use of in locating the presence of fluidized fractured regions and temperature-pressure induced phase changes in the deeper crust and upper mantle.

Magnetotelluric (MT) exploration exploits the wide bandwidth excitation of the earth by naturally occurring ionospheric current systems, to glean information from a wide depth range from a few tens of meters corresponding to 1 KHz to few hundreds of kilometers corresponding to 10^{-6} Hz at the lower end of the spectrum. Its physical basis was first provided by Cagniard (1953) who showed that the simultaneous values of orthogonal horizontal components of electric and magnetic vector pairs at the surface of a horizontally stratified earth contains all the information about the vertical distribution of electrical resistivity. Inversion of the measured values of these field

component pairs in terms of the resistivity profile thus constitutes an important step in MT exploration.

The most widely used model for inverting MT data is an earth parameterized as a stack of horizontal layers, each of a constant resistivity (Wu 1968; Patrick and Bostick 1969; Kunetz 1972), or as one characterized by a continuous variation of resistivity (Bostick 1977; Oldenburg 1979). Further details can be found in the excellent papers by Parker (1980), Parker and Whaler (1981), Varentsov (1983), Hermance (1983), Vozoff (1986), Pedersen and Hermance (1986), Chave and Booker (1987), Hohmann and Raiche (1987), Oldenburg (1990), Whittal and Oldenburg (1990).

The process of inverting an EM data set, usually of inadequate quality or density, is beset by the endemic problems of non-uniqueness and resolution common to all such ill-posed problems (Backus and Gilbert 1970; Berdichevsky and Zhdanov 1984). To circumvent this problem numerous methods, techniques and approaches resulting in robust computational algorithms have, therefore, been developed.

The EM inverse problem is essentially a non-linear one. Most existing inversion techniques deal with this by first quasi-linearizing them and then using a Newton-Raphson type of iterative scheme to obtain a solution. However, besides the pitfalls often implicit in quasi-linearization (Sabatier 1974; Anderssen 1975), these approaches require an educated guess of the model parameters as a starting point. Parker (1977) who used MT data to illustrate the discussions on the Backus-Gilbert method pointed out that a major disadvantage of reducing the essentially infinite dimensional parameter space to a finite one, results in the reduced degree of freedom in the description of unknown parameters.

In contrast to the iterative schemes certain researchers, e.g., Kunetz (1972), Weidelt (1972), Parker (1980), Fischer *et al* (1981), Parker and Whaler (1981), Barcilon (1982), and Whittal and Oldenburg (1986) have developed non-iterative schemes. Weidelt (1972) presented an inverse methodology based on the solution of Gelfand and Lavitan (1955) of the inverse Sturm-Liouville problem. Numerical implementation of this scheme is a six-stage process involving Laplace transformation and integral equation solution. Whittal and Oldenburg (1986) have implemented this scheme for four different norm definitions using either Backus-Gilbert or linear programming methods for stage three. Parker (1980) also derived an integral representation, similar to Weidelt's, and then presented three possible classes of solutions D^+, H^+ and S^+. Parker and Whaler (1981) have implemented these schemes using a two-stage process. The first stage is linear but iterative and is solved using quadratic programming method. In the second stage the conductivity profile is derived using the continued fraction representation. In the H^+ model the authors have employed the equal penetration layer thickness criterion of Kunetz (1972) and Loewenthal (1975). It may be alluded here that these schemes are theoretically rigorous, however, their implementation demands knowledge of advanced mathematical analysis and numerical methods.

These concerns motivated us to develop a non-iterative straightforward inversion scheme (SIS) for inverting MT data. This scheme is primarily based on a linear representation of the MT response function of a layered earth in terms of a power series whose coefficients are estimated using the minimum norm estimator when data are error free and the regressed minimum norm estimator when they are noisy. These coefficients are then used to obtain the layer resistivities and thicknesses through a recurrence relation developed for this purpose. The linearity of SIS algorithm significantly diminishes subjectivity as it does not require an initial model.

Furthermore, the method can be designed to yield an almost continuous resistivity depth distribution by representing the earth by a large number of closely-spaced layers. The scheme has been tested on various synthetic and field data sets with excellent results.

2. The SIS algorithm

2.1 *Forward formulation*

The surface impedance of an N-layered Earth, resting on a half space, is obtained by solving the appropriate Helmholtz equation subject to the electromagnetic boundary constraints of continuity of the tangential components at each interface. One can write the downward looking impedance Z_l (Pedersen and Hermance 1986), at the top of the l-th layer, in terms of the following recurrence relationship,

$$Z_l = z_{0l}\frac{1+R_l e^{-2v_l d_l}}{1-R_l e^{-2v_l d_l}}, \qquad l=1,2,\ldots,N-1, \tag{1}$$

where the intrinsic impedance, z_{0l}, the reflection function R_l, and the propagation constant v_l are given by

$$z_{0l} = \sqrt{\frac{j\omega\mu}{\sigma_l}},$$

$$R_l = \frac{z_{0l}-Z_{l+1}}{z_{0l}+Z_{l+1}},$$

$$v_l = \sqrt{j\omega\mu\sigma_l},$$

with d_l being the thickness of the l-th layer, ω the angular frequency, μ the magnetic permeability and $j=\sqrt{-1}$.

The impedance at the surface of the deepest half space is given by

$$Z_N = z_{oN}. \tag{2}$$

Let the thickness d_l of each layer be chosen in accordance with the equal penetration depth criterion introduced by Kunetz (1972) and Loewenthal (1975) and subsequently used by Parker (1980) to define his proxy parameter 'P' in H^+ formulation. This choice would result in $d_l/\delta_l = \alpha$, a constant. Here δ_l, the unit frequency skin depth of the l-th layer, is given by

$$\delta_l = \sqrt{\frac{\rho_l}{\pi\mu}}. \tag{3}$$

Now, defining a parameter u as

$$u = e^{-2(1+j)\alpha\sqrt{f}}, \quad \omega = 2\pi f,$$

equation (1) can be written as

$$Z_l(u)|_{\text{top}} = z_{0l}\frac{1+R_l(u)}{1-R_l(u)}. \tag{4}$$

Similarly, the upward looking impedance at the bottom of the $(l-1)$th layer, is given as,

$$Z_l(u)|_{\text{bottom}} = z_{0(l-1)} \frac{1 + R_{l-1}(u)/u}{1 - R_{l-1}(u)/u}. \tag{5}$$

The continuity of $Z_l(u)$, imposed by equating (4) and (5), yields the following recurrence relation for the reflection function

$$R_{l-1} = \frac{R_l(u) + r_{l-1}}{1 + R_l(u) r_{l-1}} u \tag{6}$$

with

$$R_{N+1}(u) = 0, \quad R_N(u) = r_N u$$

and

$$R_{N-1}(u) = \frac{r_N u + r_{N-1}}{1 + r_{N-1} r_N u} u. \tag{7}$$

Here r_1, the reflection coefficient at the l-th interface between the l-th and the $(l+1)$-th layers, is given by

$$r_l = \frac{z_{0l} - z_{0,l+1}}{z_{0l} + z_{0,l+1}} = \frac{\sqrt{\rho_{l+1}} - \sqrt{\rho_1}}{\sqrt{\rho_{l+1}} + \sqrt{\rho_1}}. \tag{8}$$

Further, as in the case of the direct current resistivity problem, (Gupta *et al* 1997) it can be shown, that

$$|u| \leq 1 \quad \text{and} \quad |R_1| < 1.$$

The reflection function, $R_1(u)$, can in turn, be expressed as a power series in u (Appendix 1) as

$$R_l(u) = \sum_{m=1}^{\infty} R_{lm} u^m. \tag{9}$$

Using this expression for $R_l(u)$ and $R_{l-1}(u)$ in equation (6) and performing some simple algebraic steps (Appendix 1) the following recurrence relation between the coefficients of the same powers of u in the power series of R_{l-1} and R_l is obtained

$$R_{l-1,1} = r_{l-1}. \tag{10}$$

$$R_{l-1,m} = r^*_{l-1} R_{l,m-1} - r_{l-1} \sum_{k=2}^{m-1} R_{l,m-k} R_{l-1,k}, \tag{11}$$

with

$$r^*_{l-1} = 1 - r^2_{l-1}.$$

The expression for $Z_l(u)$ at the top of the l-th layer can, similarly, be written as the following power series

$$Z_l(u) = \sum_{m=0}^{\infty} c_{lm} u^m. \tag{12}$$

For $m > 0$, the coefficients, c_{lm}, would be related to $R_{l,m}$ as

$$c_{lm} = R_{lm} c_{l0} + R_{l,m-1}\, c_{l1} + R_{l,m-2}\, c_{l2} + \cdots + R_{l2}\, c_{l,m-2} + r_{l1}\, c_{l,m-1}, \tag{13}$$

while

$$c_{l0} = \sqrt{\rho_l}. \tag{14}$$

Equations (8)–(14) can be employed to compute the impedance at the air-earth interface.

The widely used MT response is the apparent resistivity defined by Cagniard (1953) as

$$\rho_{a|z|} = \frac{1}{\omega\mu}|Z_l|^2. \tag{15}$$

Spies and Eggers (1986) investigated various alternative definitions of MT's apparent resistivity and found that the ones based on the real and imaginary components of the impedance were more representative. Two such definitions, given by them, are

$$\rho_{a,Re(z)} = \frac{2}{\omega\mu}[Re\ Z_l]^2, \tag{16}$$

and

$$\rho_{a,Im(z)} = \frac{2}{\omega\mu}[Im\ Z_l]^2. \tag{17}$$

Our analysis is capable of using any of these definitions, however, in order to appraise their relative merits, a discussion of equations (16) and (17) would be in order. Since the coefficients c_{lm}'s are real, both the real and imaginary components of impedance can be obtained simply by retaining in the series the real and imaginary parts of the term u^m. These can be respectively expressed as:

$$(u^m)_{Re} = e^{-m\beta} \cos m\beta. \tag{18}$$

and

$$(u^m)_{Im} = -e^{-m\beta} \sin m\beta, \tag{19}$$

where

$$\beta = 2\alpha\sqrt{f}.$$

Since c_{l0} is purely real, information about the resistivity of the l-th layer will be contained only in the real component of impedance. This would explain the superiority of the definition given by equation (16) over that of (17). It may be observed that whereas the inversion of the real component of impedance will directly lead to layer resistivities, that of the imaginary component will yield the interface reflection coefficients from which layer resistivities can be derived only when resistivity of one layer is supplied extraneously. This led us to work with the real component of impedance for MT data inversion. It may be alluded here that information about both amplitude and phase of apparent resistivity is made use of to obtain real component of impedance. The formulation is, however, presented here for the general complex case so that, if desired, even data for the imaginary component of impedance can be inverted to obtain a supplementary solution.

2.2 *Inverse formulation*

Equation (12) for the air-earth interface can be rewritten in a matrix form as,

$$Uc = Z_l \tag{20}$$

where the coefficient matrix,

$$U = \begin{bmatrix} 1 & u_1 & u_1^2 & \cdots & u_1^j & \cdots \\ 1 & u_2 & u_2^2 & \cdots & u_2^j & \cdots \\ \vdots & \vdots & \vdots & & \vdots & \cdots \\ 1 & u_i & u_i^2 & \cdots & u_i^j & \cdots \\ \vdots & \vdots & \vdots & \vdots & \vdots & \\ 1 & u_m & u_m^2 & \cdots & u_m^j & \cdots \end{bmatrix}$$

the unknown column vector,

$$c = [c_{10}, c_{11}, c_{12}, \ldots, c_{lm}, \ldots]^t,$$

and the known impedance vector,

$$Z_l = [Z_1(u_1), Z_1(u_2), \ldots, Z_1(u_M)]^t.$$

Here, the superscript t stands for the matrix transpose operation. The minimum norm solution of equation (20) can be written as:

$$\hat{c} = U^t W, \tag{21}$$

with

$$W = [UU^t]^{-1} Z_l.$$

It may be emphasized here that no truncation is employed in the evaluation of ij-th element of UU^t which is obtained as given below

$$(UU^t)_{ij} = \sum_{k=0}^{\infty} (u_i u_j)^k$$

$$= \frac{1}{1 - u_i u_j}.$$

The estimated solution vector c is used to assess the quality of inverse solution by first computing the response vector

$$\hat{Z}_l = U\hat{c}$$

and then the misfit parameters ε_a and ε_r computed respectively as the absolute root mean square (rms) error and the relative rms error between the observed data Z_l and the predicted data $\hat{Z}_l$ as given below

$$\varepsilon_a^2 = \sum_{i=1}^{M} [Z_{li} - \hat{Z}_{li}]^2 / M,$$

$$\varepsilon_r^2 = \sum_{i=1}^{M} [(Z_{li} - \hat{Z}_{li})/Z_{li}]^2 / M.$$

It may be stressed here that equation (21) will yield a unique solution only when equation (20) is consistent and the matrix U full rank. However, in the case of field data, where the inadequacy and the random errors of measurement make consistency impossible, one may seek a regularized minimum norm solution given by

$$\hat{c} = U^t(UU^t + E)^{-1} Z_l, \tag{22}$$

where E is the data error covariance matrix. In case the error covariance matrix is not available it can be approximated by $e^2 I$, e being the average noise to signal ratio.

Equation (21) provides that

$$c_{l0} = \sum_{l=1}^{N} w_l = \sqrt{\rho_l}. \tag{23}$$

$$c_{lm} = \sum_{1} u_l^m w_l, \quad m > 0. \tag{24}$$

It may be added here that N is a sufficiently large (between 1000–2000) number so that the contribution of remainder terms of the power series is negligible. The coefficients R_{lm} can be related to c_{lm} through equation (13) as,

$$2\sqrt{\rho_l} R_{lm} = c_{lm} R_{l0} - c_{l,m-1} R_{11} - c_{l,m-2} R_{12} - \cdots - c_{12} R_{l,m-2} - c_{11} R_{l,m-1}. \tag{25}$$

Consequently, the following inverse recurrence relation is developed through equation (11)

$$R_{l,m-1} = \frac{1}{r^*_{l-1}} \left[R_{l-1,m} + r_{l-1} \sum_{k=2}^{m-1} R_{l,m-k} R_{l-1,k} \right]. \tag{26}$$

Thus the various reflection coefficients, r_l and the layer resistivities ρ_l, can be obtained as

$$r_l = R_{11},$$
$$\rho_{l+1} = \left[\frac{1 + R_{l1}}{1 - R_{l1}} \right]^2 \rho_l. \tag{27}$$

Once the resistivity of the l-th layer is obtained, its thickness can readily be computed through the expression

$$d_l = \alpha \delta_l = \alpha \sqrt{\rho_l / \pi \mu}. \tag{28}$$

Thus the solution of the inverse MT problem is completely obtained through equations (21–28), in a linear fashion, without any initial model. However, the value of α has to be judiciously chosen keeping in mind the expected thickness and resistivity of the target layer which ought to be resolved.

In order to estimate the quality of inverted conductivity model, the misfit ε_t between its response $\hat{Z}_l$ and the observation Z_l can be computed in a manner similar to that used for ε_r as

$$\varepsilon_t^2 = \sum_{i=1}^{M} \frac{[(Z_{li} - \hat{Z}_{li})/Z_{li}]^2}{M}.$$

3. Numerical consideration

The vector c, obtained as the solution of equation (20) or (22), can be looked upon as the initial condition of an initial value problem. This means that as the solution is continued downward, the error in c will propagate and may get enhanced. This error propagation may sometimes lead to non-physical reflection coefficients lying outside the $(-1, 1)$ interval. This should always be taken as a warning signal, that no further downward continuation of conductivity profile is possible. Such eventuality will occur only if the regression parameter is not able to account for the error in data and/or the 1-D model is incompatible to the real conductivity distribution. A possible way out is to use higher regression parameter value. The higher regression parameter value will lead to the increased misfit and blurred conductivity profile. Further, for smooth functioning of the SIS algorithm, the inverted reflection coefficients should be approximated as zero whenever it lies within a prescribed infinitesimal interval. In the present study this interval is $-0{\cdot}01$ to $0{\cdot}01$.

4. Model studies

The SIS algorithm was tested on several synthetic as well as field data sets. The results of four synthetic data sets and two field data sets are discussed below. The synthetic models considered here have been specially chosen to highlight efficacy of the SIS algorithm.

4.1 *Model 1*

This is the four-layer model designed by Porstendorfer (1975) to study the limitations of the MT method in deciphering highly resistive layers buried underneath conducting layers. It represents a typical thick sedimentary basin overlying a highly resistive (10^4 ohm-m) substratum (for instance crystalline rock). The first layer in this model is well conducting: $\rho_1 = 2$ ohm-m, and thickness $d_1 = 2000$ m. The second layer is an insulating salt layer: $\rho_2 = 10000$ ohm-m and $d_2 = 1000$ m, and the third layer comprises sediments of medium resistivity: $\rho_3 = 20$ ohm-m and $d_3 = 6{,}500$ m. Forward computations were carried out using equations (10), (11) and (12) to obtain the real part of impedance at 26 data points for a period ranging from 10^{-2} to 10^3s. Equation (16) was then used to compute the apparent resistivity values. The unit of layer thickness was chosen to be 1000 m, which fixed the value of α, the layer thickness unit in terms of the layer skin depth, at 0·01987. As expected the highly resistive layers are weakly defined in the apparent resistivity curve. For carrying out the inversion, a 650-layer model with constant α was selected. Equations (26), (27) and (28) were then used to estimate the resistivity variations. The results are shown in figure 1. It may be observed that, in accordance with the apparent resistivity curve, the inverse solution also reproduces the true signatures only of the conducting layers: 1 and 3, masking completely the highly resistive layers 2 and 4. The screening effect of resistivity of the first layer on inverse solutions, was therfore, further studied by changing its resistivity to 20 ohm-m and 200 ohm-m, leaving all other layer parameters unchanged. The apparent resistivity curves as well as the inverted model for these two cases are also shown in figure 1. When the resistivity of the first layer is increased, both the resistive layers 2 and 4, become visible.

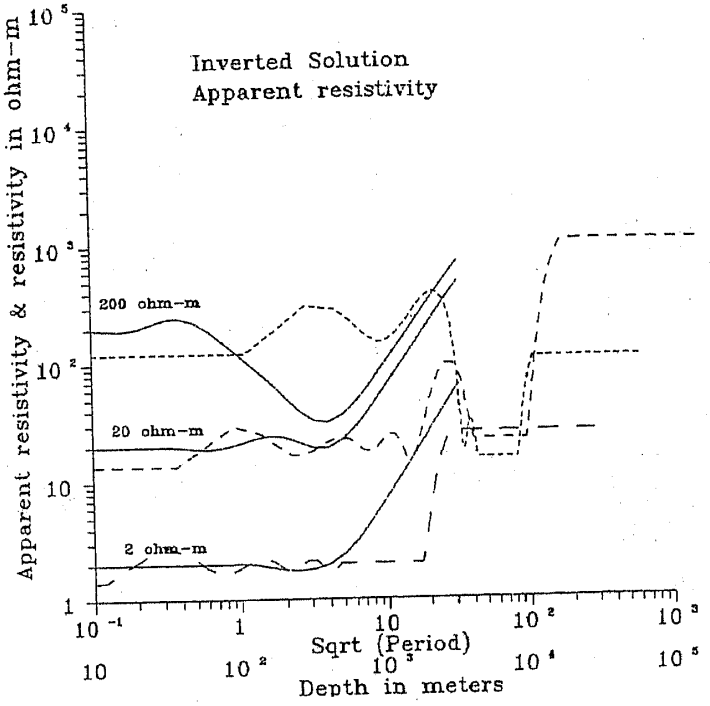

Figure 1. Apparent resistivity curves and corresponding inverse solutions for the three cases of model 1. The factors 2, 20 and 200 refer to true resistivities of first layer.

However, layer 4 is prominent in the $\rho_1 = 200$ ohm-m case while layer 2 is in the $\rho_1 = 20$ ohm-m case. The conducting layer 3 is well represented in both the cases. Once the high frequency oscillations are averaged out the smooth model is quite close to the true one except for the highly resistive layers 2 and 4 whose resistivities are always grossly underestimated. Further, the relative rms errors, ε_r and ε_t, in all three cases were found to be of the order of 10^{-9} and 10^{-1} respectively.

4.2 *Model 2*

A study of the influence on the inverted solution of the data error, the regression parameter (e^2) and of the layer thickness unit α was carried out by considering the five layer Model of Oldenburg (1990): $\rho_1 = 250$ ohm-m, $d_1 = 1000$ m; $\rho_2 = 25$ ohm-m, $d_2 = 2000$ m; $\rho_3 = 100$ ohm-m, $d_3 = 3000$ m; $\rho_4 = 10$ ohm-m, $d_4 = 4000$ m; $\rho_5 = 25$ ohm-m. The real component of impedance as well as the apparent resistivities were computed as before for 26 values of the period. The minimum layer thickness was chosen to be 500 m, thereby fixing $\alpha = 0{\cdot}063$. The number of layers assumed for the inverse model was 100. The error-free inverse solution along with the true model and the apparent resistivity curve is shown in figure 2(a). The rms errors ε_r and ε_t in this case were $1{\cdot}5 \times 10^{-10}$ and 0·059 respectively. From the inverse solution plot it is evident that all the five layers have been adequately resolved.

The effect of data error on inverted model was studied by generating four data sets corrupted with 0·1, 1, 10 and 25% random Gaussian noise. The corresponding inverted solutions, plotted in figure 2(b), were obtained using the regression parameter (e^2) values equal to the respective error percentage. The rms error ε_r values in the four cases

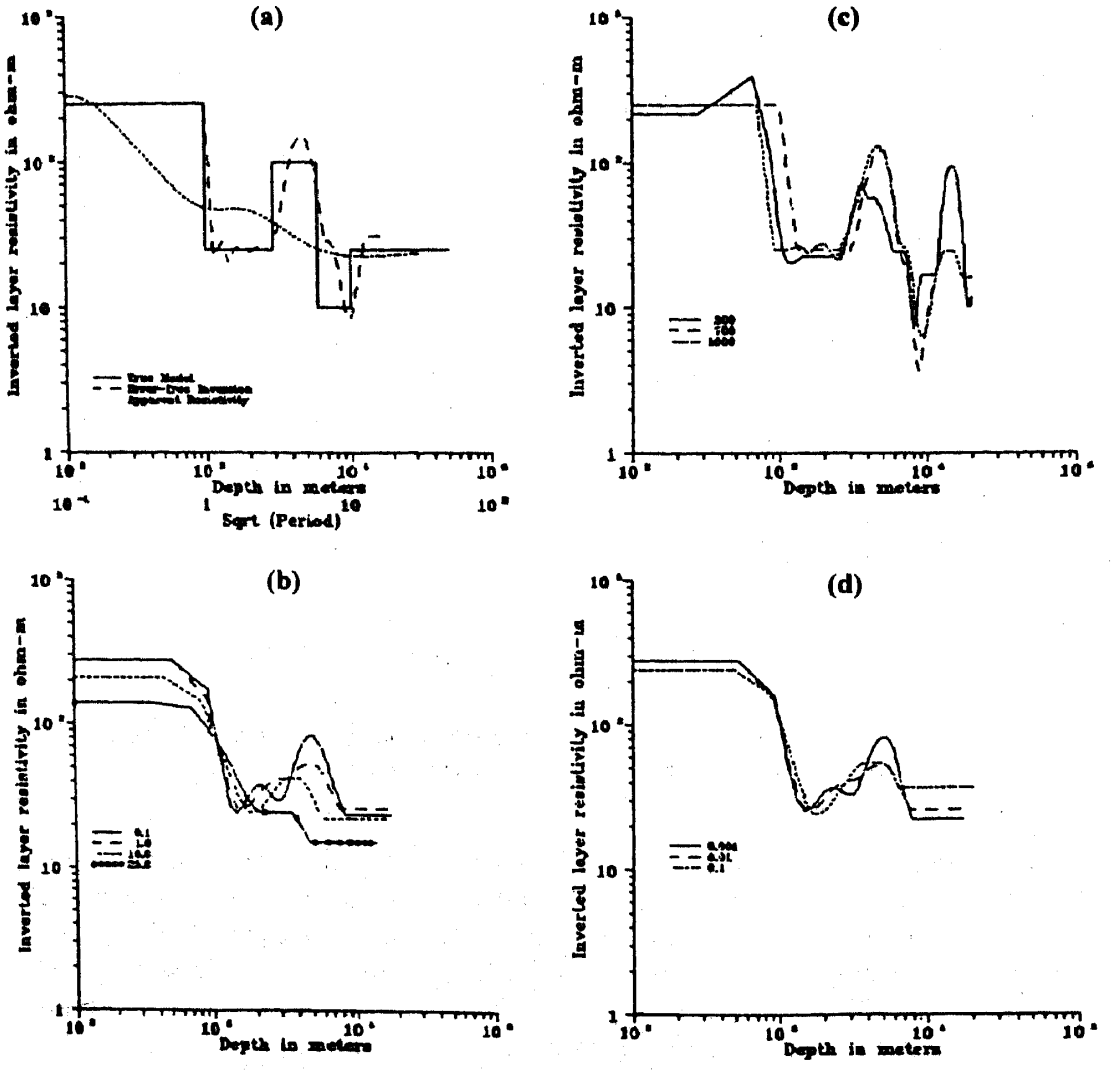

Figure 2. The stability study of SIS on model 2: (**a**) true model, its apparent resistivity curve and error free inverted model, (**b**) the inverted models of the responses corrupted with 0.1, 1.0, 10.0 and the error free inverted model, (**c**) The inverted models of the error free response for layer thickness unit values 300, 700 and 1000 m, (**d**) The inverted models of the 0.001 per cent error corrupted response for the regression parameter e^2 values 0.001, 0.01 and 0.1.

were 0·0021, 0·008, 0·08 and 0·217 respectively. The corresponding ε_t values were 0·113, 0·117, 0·116 and 0·237. It may be observed that in all the four cases the highly conducting layer 4 could not be retrieved while the magnitude of the peak values of layer resistivities got reduced for layers 1 and 3, a feature which became more prominent for the higher noise levels. When the noise level was 25%, even layer 3 could not be perceived. It may, therefore, be argued that error in the inverse solutions is contained within acceptable limits if the data has up to 10% noise.

The effect on inverted model of the variation in magnitude of layer thickness unit was studied by inverting the error-free data for the minimum layer thickness equal to 300 m, 700 m and 1000 m corresponding to α values ·038, ·088 and ·126 respectively. The inverted solutions are presented in figure 2(c). It is evident that in all the three cases the basic features are retrieved at it was in the case of 500 m. It may be added here that for

layer thickness unit 300 m the solution oscillates wildly at depths greater than 10 km which is well beyond the target depth. The ε_r values in three cases were $3{\cdot}86 \times 10^{-7}$, $1{\cdot}73 \times 10^{-12}$ and $1{\cdot}81 \times 10^{-12}$ respectively while the corresponding ε_t values were 0·058, 0·045 and 0·098.

Lastly, the effect of regression parameter (e^2) variation on the inverse solution was studied on the response corrupted with 0·1 per cent noise. The e^2 values used in these cases were ·001, ·01 and ·1. The corresponding rms error ε_r values were $5{\cdot}96 \times 10^{-3}$, $7{\cdot}97 \times 10^{-3}$ and $2{\cdot}46 \times 10^{-2}$ respectively while the ε_t values were 0·104, 0·117 and 0·197. The inverse solutions are plotted in figure 2(d) which confirms the expectations that the retrieved solution features get smoothened as e^2 values increases.

4.3 *Model 3*

This is an eight-layer model taken from Manglik (1988). It comprises alternate sequence of highly conducting and moderately resistive layers: $\rho_1 = 7{\cdot}389$ ohm-m, $d_1 = 10$ m; $\rho_2 = 1{\cdot}0$ ohm-m, $d_2 = 20$ m; $\rho_3 = 4{\cdot}482$ ohm-m, $d_3 = 40$ m; $\rho_4 = 1{\cdot}649$ ohm-m, $d_4 = 30$ m; $\rho_5 = 148{\cdot}4$ ohm-m, $d_5 = 200$ m; $\rho_6 = 2{\cdot}718$ ohm-m, $d_6 = 400$ m; $\rho_7 = 20{\cdot}09$ ohm-m, $d_7 = 2300$ m; $\rho_8 = 1{\cdot}649$ ohm-m. Basic synthetic data used in the inversion scheme, real component of the impedance, were computed for 25 values of the period from 10^{-3} to 10^2s using a minimum layer thickness of 10 m corresponding to $\alpha = 0{\cdot}0073$. For graphical presentation the apparent resistivity values were also computed. The model, its apparent resistivity response as well as the SIS inverse solution are presented in figure 3(b). For comparison, the inverted model obtained by Manglik (1988), using Oldenburg's (1979) formulation of the Backus and Gilbert Method (BGM), is shown in figure 3(a). From this it can be seen that the BGM inverted model amalgamates the second, third and fourth layer features into one, completely missing the thin highly conducting fourth layer. The SIS inverted model on the other hand, distinctly resolves all the features of these layers. Further, in the BGM inverted model the resistivity of the last layer exhibits spurious variations. This last conducting layer is in fact not sensed at all in the SIS solution but this is not a serious disadvantage as this value can be easily estimated from the right asymptote of the apparent resistivity curve. The rms error in SIS and BGM cases were $1{\cdot}82 \times 10^{-11}$ and $4{\cdot}6 \times 10^{-3}$ respectively. The rms error ε_t in SIS was 0·231.

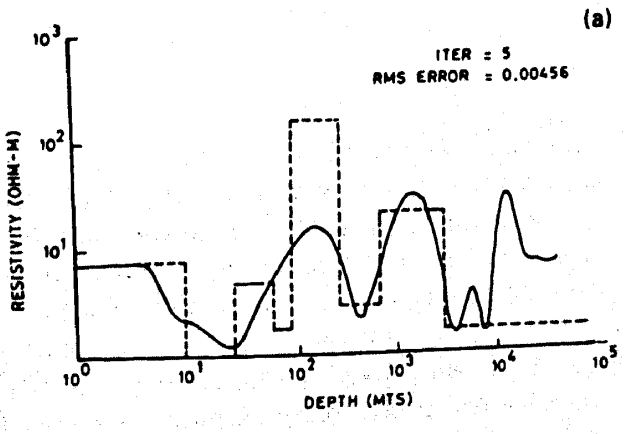

Figure 3(a). Backus-Gilbert inversion of MT data computed for model 3 (taken from Manglik 1988).

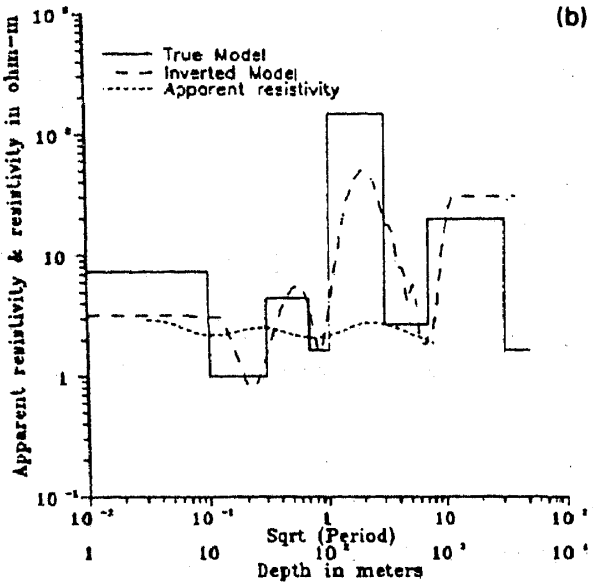

Figure 3(b). Apparent resistivity values, true model and SIS solution of model 3.

4.4 *Model 4*

This four-layer model, taken from Sri Niwas and Kumar (1991), represents a geological situation prevailing in the Saurashtra region of western India and is based on the interpretation of dipole electrical sounding curves. Its parameters are: $\rho_1 = 20$ ohm-m, $d_1 = 50$ m; $\rho_2 = 200$ ohm-m, $d_2 = 3000$ m; $\rho_3 = 10$ ohm-m, $d_3 = 5000$ m and $\rho_4 = 5000$ ohm-m. The real component of impedance as well as the apparent resistivity were obtained for the 25 period values ranging from 10^{-2}–10^{3}s using a minimum layer thickness unit of 250 m ($\alpha = 0{\cdot}0222$). The model, the apparent resistivity curve, the SIS inverted model, the model obtained using the Ridge Regression Method (RRM) (Sri Niwas and Kumar 1991) and one obtained using Occam's method (OM) (Naresh Kumar 1989) are reproduced in figure 4. The rms errors ε_r and ε_t in the SIS solution were $1{\cdot}93 \times 10^{-9}$ and 0·165. It is clear that on the whole SIS solution is best while the last layer is best estimated by RRM. It may be added here that the RRM estimates were obtained using the initial guess model–$\rho_1 = 15$ ohm-m, $d_1 = 100$ m; $\rho_2 = 300$ ohm-m, $d_2 = 2500$ m; $\rho_3 = 20$ ohm-m, $d_3 = 4000$ m; $\rho_4 = 4000$ ohm-m which was quite close to the true model.

4.5 *Field data 1*

The first field data set analysed here was procured and inverted by Larsen (1975). It comprised twelve complex admittance values which were taken from Parker and Whaler (1981) (PW), who reinterpreted the data set using their H^+ inversion scheme. PW have stated that Larsen (1975) as well as they themselves were unable to find any one-dimensional conductivity model that could account for all the twelve response values. However, when only the seven values corresponding to larger time-periods were used, they could invert the data for 1-D models. From the complete data set we computed the twelve real components of the impedance values and used these as our data. While inverting the complete 12 frequency data set we faced the problem of non-physical reflection coefficient with magnitude > 1,

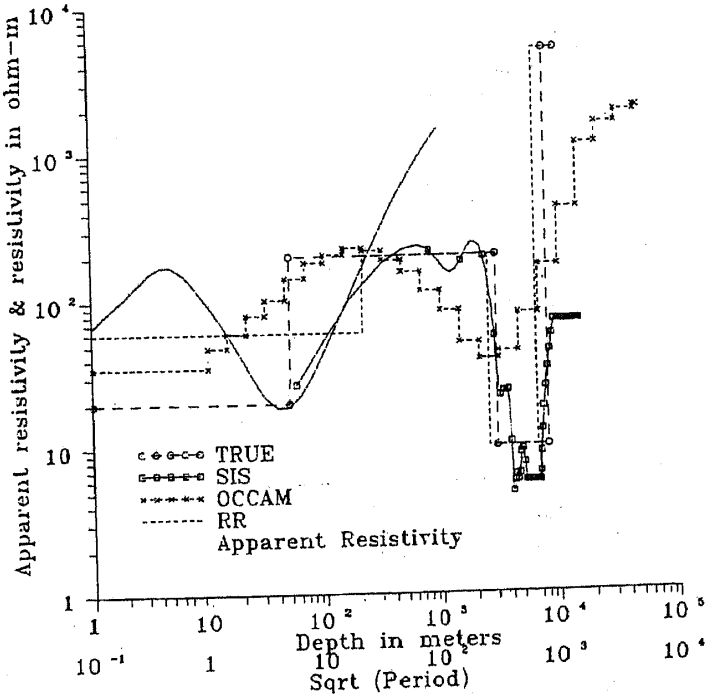

Figure 4. True model 4, its apparent resistivity and the inverted solutions obtained using SIS, Ridge Regression and Occam's methods.

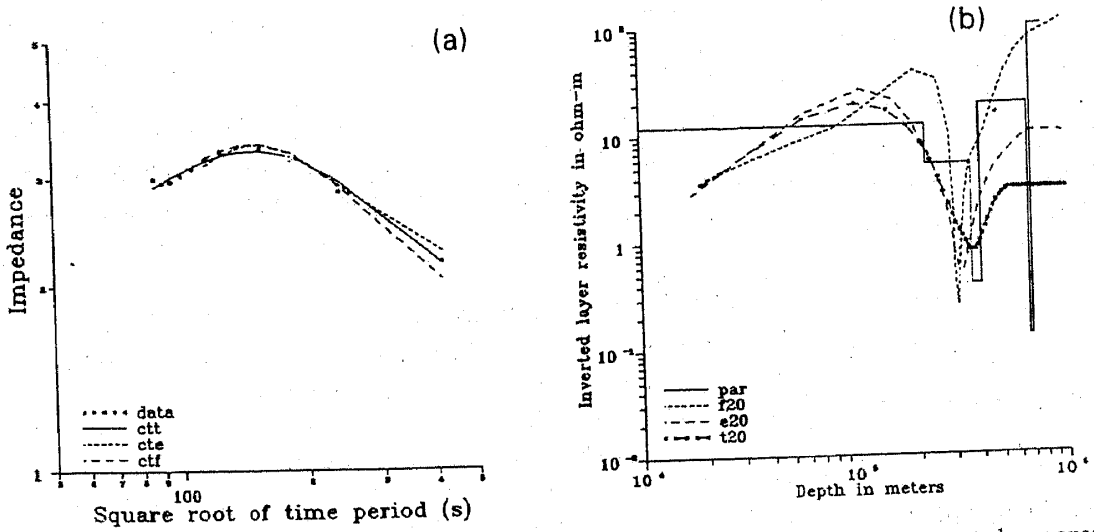

Figure 5(a). Real component of impedance observations (data) and the computed responses *ctt*, *cte* and *ctf* of inverted models *t* 20, *e* 20 and *f* 20 respectively. **(b).** Inversion of Larsen's data (1975): par-the 7 data H^+ solution of Parker and Whaler (1981), *f* 20 and *e* 20 the SIS solutions for 7 data with $e^2 = 0.0$ and 0.001 respectively and *t* 20 the 12 data SIS solution for $e^2 = 0.01$.

meaning thereby that either the data are erroneous or the 1-D model is not representing the real situation. When we rerun the program with regression parameter $e^2 = 0{\cdot}01$ a useful 1-D model *t* 20, is achieved. The errors after the two stages were $\varepsilon_r = 0{\cdot}016$ and $\varepsilon_t = 0{\cdot}018$. It means that SIS can better interpret data generated by real situations which deviates from 1-D models. To gauge the usefulness of this inverted model the seven frequency data set was then inverted without and with 0·001

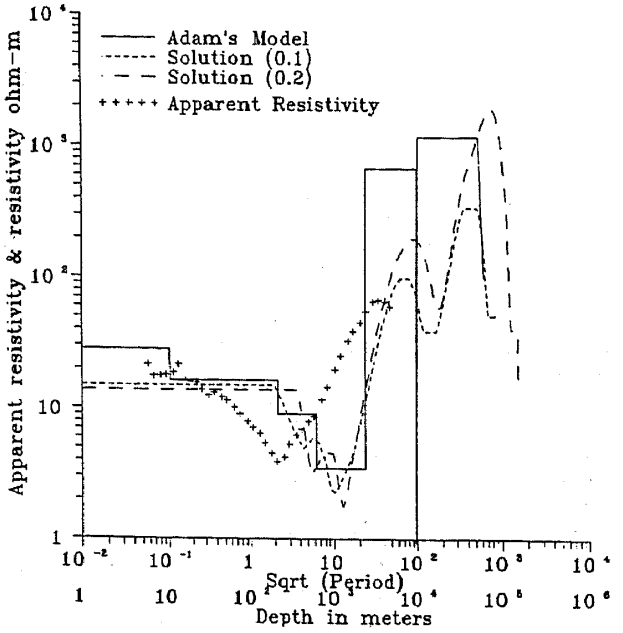

Figure 6. The apparent resistivity curve from Panonian Basin, Hungary, its Ridge Regression Solution (after Adam 1990) and the two SIS solution for $\alpha = 0.1$ and 0.2.

regression values. The resulting model $f20$ and $e20$ together with $t20$ and the model of par are plotted in figure 5(b) while the fit of the computed responses of $f20$, $e20$ and $t20$ are shown in figure 5(a) as curves *ctf*, *cte* and *ctt* respectively. The rms error parameter for $f20$ were $\varepsilon_r = 1{\cdot}13 \times 10^{-11}$, $\varepsilon_t = 0{\cdot}0242$ and for $e20$ were 0·00043 and 0·028 respectively. It is interesting to note that all the three inverted models viz., $t20$, $f20$, $e20$ are depicting the first conducting zone obtained by PW very closely, however, the second 22 km conducting zone indicated by PW at a depth of 669 km is not seen.

4.6 *Field data 2*

Lastly, we applied SIS to invert a field data set from Panonian basin in Hungary provided by Adam (1990). For SIS inversion, the real component of impedance was computed using the apparent resistivity and phase data of Adam (1990). The apparent resistivity curve, Adam's RRM inverted model and the SIS solution with two different values of α, 0·1 and 0·2, are presented in figure 6. In SIS the regularization parameter e^2 was taken as 0·01 assuming 1% noise. The rms error ε_t values in the solutions for $\alpha = 0{\cdot}1$ and 0·2 were 0·029 and 0·044 respectively while the corresponding ε_t values were 0·068 and 0·096. All the anticipated features of the model have been well retrieved in both the SIS solutions. However, the resistive layers are more prominent in the solution corresponding to $\alpha = 0{\cdot}2$. It must again be stressed here that unlike Adam's RRM inversion, where an initial model – $\rho_1 = 31{\cdot}04$ ohm m, $d_1 = 11$ m; $\rho_2 = 16{\cdot}0$ ohm m, $d_2 = 222$ m; $\rho_3 = 8{\cdot}22$ ohm m, $d_3 = 428$ m; $\rho_4 = 3{\cdot}36$ ohm m, $d_4 = 1723$ m; $\rho_5 = 680$ ohm m, $d_5 = 12480$ m; $\rho_6 = 0{\cdot}00350$ ohm m, $d_6 = 247$ m; $\rho_7 = 125$ ohm m, $d_7 = 72220$ m and $\rho_8 = 40{\cdot}76$ ohm m–very close to the true one was assumed, no such arbitrariness was needed to obtain the SIS solution.

5. Conclusions

Based on a sound mathematical treatment, and having been successfully tested on diverse models, the SIS algorithm for inverting MT data has been demonstrated to be an efficient and robust algorithm of high resolving power. In contrast to the conventional use of amplitude or phase data of impedance function, the SIS employs its real or imaginary components. Being linear, SIS is non-iterative and it does not require an initial guess model. It is therefore, free from the disadvantages of quasi-linearized iterative schemes. Further, it provides a nearly continuous resistivity variation with depth as a very large number of closely-spaced layers can be assumed to parameterize the model. The continuous solution so obtained can then be used to obtain the gross layered earth models by averaging over any desired depth range. The rms error ε_r and ε_t are, for field or erroneous synthetic data, of the order of error in data. In cases where the inverted model is not able to retrieve deeper layers, the computed higher time period response is not correct and this results in a higher ε_t value. It may be added that the imaginary component inversion is more sensitive to the surface features and hence may be used for studying the topographic effects. The only concernable limitation of SIS is that in its present form it is unable to fruitfully use *a priori* information.

Acknowledgement

This work was carried out under a CSIR, Government of India research project. The authors are thankful to Anupama Rastogi and Yesh Pal Singh for their help in computations.

Appendix 1

Derivation of recurrence relation (11)

In order to understand the structure of relation (6) let us explicitly write the expressions for reflection functions $R_l(u)$ for $l = N+1$, N and $N-1$ as power series in u.

$$R_{N+1}(u) = 0 = \sum_m R_{N+1,m} u^m \quad \text{with} \quad R_{N+1,m} = 0 \; \forall \; m.$$

$$R_N(u) = r_N u = \sum_m R_{Nm} u^m \quad \text{with} \quad R_{N1} = r_N \quad \text{and} \quad R_{Nm} = 0 \; \forall \; m > 1.$$

$$\begin{aligned} R_{N-1}(u) &= \frac{R_N(u) + r_{N-1}}{1 + R_N(u) r_{N-1}} u, \\ &= u(r_N u + r_{N-1})(1 + r_{N-1} r_N u)^{-1}, \\ &= r_{N-1} u + r_N (1 - r_{N-1}^2) \sum_{m=0}^{\infty} (-r_{N-1} r_N)^m u^{m+2}, \\ &= \sum_{m=1}^{\infty} R_{N-1,m} u^m, \end{aligned}$$

with

$$R_{N-1,1} = r_{N-1} \quad \text{and} \quad R_{N-1,m} = r_N r^*_{N-1}(-r_{N-1}r_N)^{m-2} \; \forall \; m > 1.$$

Here

$$r^*_{N-1} = (1 - r^2_{N-1}).$$

This suggests that the function $R_l(u)$ and $R_{l-1}(u)$ appearing in relation (6) can be expressed as

$$R_{l-1}(u) = \sum_m R_{l-1,m}\, u^m,$$

$$R_l(u) = \sum R_{l,m} u^m.$$

Using these relations in equation (6) and cross-multiplying we get

$$\sum_{m=1}^{\infty} R_{l-1,m}u^m + r_{l-1}\sum_{m=1}^{\infty} R_{l-1,m}u^m \sum_{k=1}^{\infty} R_{lk}u^k = \sum_{m=1}^{\infty} R_{lm}u^{m+1} + r_{l-1}u$$

$$\text{or } (R_{l-1,1} - r_{l-1})\,u + \sum_{m=2}^{\infty}\left[R_{l-1,m} - R_{l,m-1} + r_{l-1}\sum_{k=1}^{m-1} R_{l-1,k}R_{l,m-k}\right]u^m = 0$$

$$\text{or } (R_{l-1,1} - r_{l-1})u + \sum_{m=2}^{\infty}\left[R_{l-1,m} - (1 - r_{l-1}R_{l-1,1}R_{l,m-1} + r_{l-1}\sum_{k=2}^{m-1} R_{l-1,k}R_{l,m-k}\right]u^m = 0.$$

Since this relationship is valid for all possible values of u, equating the coefficients of various powers of u to zero we get

$$R_{l-1,1} = r_{l-1}.$$

$$R_{l-1,2} = (1 - r^2_{l-1})R_{l1} = r^*_{l-1}R_{l1}.$$

$$R_{l-1,m} = r^*_{l-1}R_{l,m-1} - r_{l-1}\sum_{k=1}^{m-1} R_{l-1,k}R_{l,m-k} \quad m > 1.$$

References

Adam A 1990 Personal communication.

Anderssen R S 1975 On the inversion of global electromagnetic data; *Phys. Earth Planet. Int.* **10**, 292–298

Backus G E and Gilbert J E 1970 Uniqueness in the inversion of inaccurate gross earth data; *Philos. Trans. R. Soc. London*, **266**, 123–192

Barcilon V 1982 An explicit method for solving the geomagnetic induction problem; *Geophys. J. R. Astron. Soc.* **70**, 205–215

Berdichevsky M N and Zhdanov M S 1984, *Advanced theory of deep geomagnetic sounding*, Elsevier.

Bostick F X Jr 1977 A simple almost exact method of MT analysis; in *Workshop on electrical methods in geothermal exploration* (Univ. of Utah, Salt Lake City)

Cagniard L 1953 Basic theory of the magnetotelluric method of geophysical Prospecting; *Geophysics*, **18**, 605–635

Chave A D and Booker J R 1987 Electromagnetic induction studies; *Rev. Geophys.* **25**, 989–1003

Fischer G, Schnegg P A, Peuiron M and Liquang B V 1981 An analytic one-dimensional magnetotelluric inversion scheme; *Geophys. J. R. Astron. Soc.* **67**, 257–278

Gelfand I M and Levitan R M 1955 On the determination of a differential equation by its spectral function; *Am. Math. Soc. Trans. Series 2*, **1**, 253–304

Gupta P K, Sri Niwas and Gaur V K 1996 Straightforward inversion of vertical electrical sounding data; *Geophysical Prospecting* (communicated)

Hermance J F 1983 Electromagnetic induction studies; *Rev. Geophys.* **21**, 652–664

Hohmann, G W and Raiche, A P 1988 Inversion of controlled source electromagnetic data, in Electromagnetic methods in applied geophysics Nabhighian, M N (ed), *Theory, Soc. Expl. Geophys.* Vol.1

Kunetz G 1972 Processing and interpretation of magnetotelluric soundings; *Geophysics*, **37**, 1005–1021

Larsen J C 1975 Low frequency (0.1–0.6c pd) electromagnetic study of deep mantle electrical conductivity beneath the Hawaiian islands; *Geophys. J. R. Astron. Soc.* **43**, 17–46

Loewenthal D 1975 Theoretical uniqueness of the magnetotelluric inverse problem for equal penetration discretizable models; *Geophys. J. R. Astron. Soc.* **43**, 897–903

Manglik A 1988 Backus-Gilbert magnetotelluric inversion, M.Tech. Dissertation, University of Roorkee, Roorkee

Naresh Kumar 1989 Occam's inversion of geoelectrical data of Saurashtra region, India: M. Tech Dissertation, University of Roorkee

Oldenburg D W 1979 One-dimensional inversion of natural source magnetotelluric observations; *Geophysics.* **44**, 1218–1244

Oldenburg D W 1990 Inversion of electromagnetic data: An overview of new techniques; *Surv. Geophys.* **11**, 231–170

Parker R L 1977 Understanding inverse theory; *Annu. Rev. Earth Planet. Sci.* **5**, 35–64

Parker R L 1980 The inverse problem of electromagnetic induction: Existence and construction of solutions based upon incomplete data; *J. Geophys. Res.* **85**, 4421–4428

Parker R L and Whaler K A 1981 Numerical methods for establishing solutions to the inverse problem of electromagnetic induction, *J. Geophys. Res.* **86**, 9574–9584

Patrick F W and Bostick F X Jr 1969 Magnetotelluric modelling technique, Rep. 59; *Elec. Geophys. Res. Lab.* University of Texas, Austin

Pedersen J and Hermance J F 1986 Least square inversion of one-dimensional magnetotelluric data: An assessment of procedures employed by Brown University; *Surv. Geophys.* **8**, 187–231

Porstendorfer G 1975 Principles of magnetotelluric prospecting (Berlin; Borntraeger)

Sabatier P C 1974 Remarks on approximation methods in geophysical inverse problem; *Proc R. Soc. London*, **A 337**, 49–71

Spies B R and Eggers D E 1986 The use and misuse of apparent resistivity in electromagnetic method; *Geophysics* **51**, 1462–1471

Sri Niwas and Kumar P 1991 Resolving power of direct current and magnetotelluric resistivity soundings in exploring thick sedimentary horizons; *Acta. Geod. Geoph. Mont. Hung.* **26**, 435–452

Varentsov I V M 1983 Modern trends in the solution of forward and inverse 3-D electromagnetic problems, *Geophys. Surv.* **6**, 55–78

Vozoff K 1986 Magnetotelluric methods; Geophysical reprint series No. **5**, *Soc. Expl. Geophys.*

Weidelt P 1972 The inverse problem of geomagnetic induction; *Z. fur. Geophys.* **38**, 257–289

Whittall K P and Oldenburg D W 1986 Inversion of magnetotelluric data using a practical inverse scattering formulation; *Geophysics* **51**, 383–395

Whittall K P and Oldenburg D W 1990 Inversion of magnetotelluric data over one-dimensional earth, in SEG Monograph, edited by P Wannamaker

Wu F T 1968 The inverse problems of magnetotelluric sounding; *Geophysics*, **33**, 972–978